
1 Dual Impact of Global Urban Heat on Mortality

2

3 Shasha Wang¹, Wenfeng Zhan^{1,2*}, Bingbing Zhou³, Shilu Tong^{4,5}, TC Chakraborty⁶,
4 Zihua Wang⁷, Kangning Huang⁸, Huilin Du¹, Ariane Middel⁹, Jiufeng Li¹, Zihan
5 Liu¹, Long Li¹, Fan Huang¹, and Manchun Li¹⁰

6

7 1. Jiangsu Provincial Key Laboratory of Geographic Information Science and
8 Technology, International Institute for Earth System Science, Nanjing University,
9 Nanjing, Jiangsu, China

10 2. Jiangsu Center for Collaborative Innovation in Geographical Information
11 Resource Development and Application, Nanjing, China

12 3. School of International Affairs and Public Administration, Ocean University of
13 China, Qingdao, China

14 4. National Institute of Environmental Health Chinese Center for Disease Control
15 and Prevention Beijing, China

16 5. School of Public Health and Social Work, Queensland University of Technology,
17 Brisbane, Australia

18 6. Atmospheric Sciences and Global Change Division, Pacific Northwest National
19 Laboratory, Richland, Washington, USA

20 7. School of Sustainable Engineering and the Built Environment, Arizona State
21 University, Tempe, Arizona, USA

22 8. New York University Shanghai, Shanghai, China

23 9. Global Institute of Sustainability and Innovation, Arizona State University,
24 Tempe, Arizona, USA

25 10. School of Geography and Ocean Science, Nanjing University, Nanjing, Jiangsu,
26 China

27

28 **CONTACT INFORMATION**

29 * **Corresponding author:** W. Zhan (zhanwenfeng@nju.edu.cn), Nanjing University
30 at Xianlin Campus, No. 163 Xianlin Avenue, Qixia District, Nanjing, Jiangsu 210023,
31 China.

32

33

34 **ABSTRACT**

35 Urban heat exacerbates heat-related mortality in cities during the hot season, but its
36 potential to reduce cold-related mortality during cold spells is often overlooked. A
37 comprehensive evaluation of the duality of urban heat impacts on temperature-related
38 mortality globally remains lacking. Here we quantitatively assess the beneficial and
39 detrimental impacts of the urban heat island (UHI) effect and associated urban cooling
40 strategies on temperature-related mortality in over 3,000 cities worldwide by
41 integrating multi-source remote sensing estimates, climate data, and empirical
42 mortality-temperature relationships. We find that the UHI effect reduces global cold-
43 related mortality, surpassing the increase in heat-related mortality by more than
44 fourfold. We show that widely implemented urban cooling strategies, including green
45 and reflective infrastructure, benefit about 20% of tropical cities but have a
46 detrimental net effect in most of the world's cities. We propose seasonal adjustments
47 to roof albedo as an actionable strategy to reduce heat- and cold-related mortality. Our
48 findings highlight that urban heat can protect against mortality in most non-tropical
49 cities in the cold season, emphasizing the importance of seasonally and place-based
50 adaptive UHI mitigation strategies to reduce temperature-related mortality.

51

52

53 **MAIN**

54 The health and well-being of urban populations are central to achieving the

55 Sustainable Development Goals (SDGs) set forth by the United Nations (SDG-11:

56 Sustainable Cities and Communities)¹. With Earth's ongoing urbanization and rapid

57 warming, urban overheating has become a significant threat to human health,

58 affecting the mortality and morbidity rates in cities globally²⁻⁵. One of the

59 contributing factors to increased human heat exposure is the urban heat island (UHI)

60 effect, a phenomenon characterized by higher ambient temperatures in cities

61 compared to their rural surroundings⁶. Similar to numerous other anthropogenic

62 environmental and ecological alterations⁷, the UHI effect exhibits a dual impact. It

63 exacerbates heat-related mortality, particularly during periods of elevated

64 temperatures⁸⁻¹⁰, while simultaneously reducing cold-related mortality in cooler

65 conditions¹¹⁻¹⁴, as indicated by the broadly recognized J- or U-shaped temperature-

66 mortality relationship curve (refer to Fig. 1). In the context of rapid urbanization and

67 climate change, it is critical to investigate the dual (beneficial and detrimental)

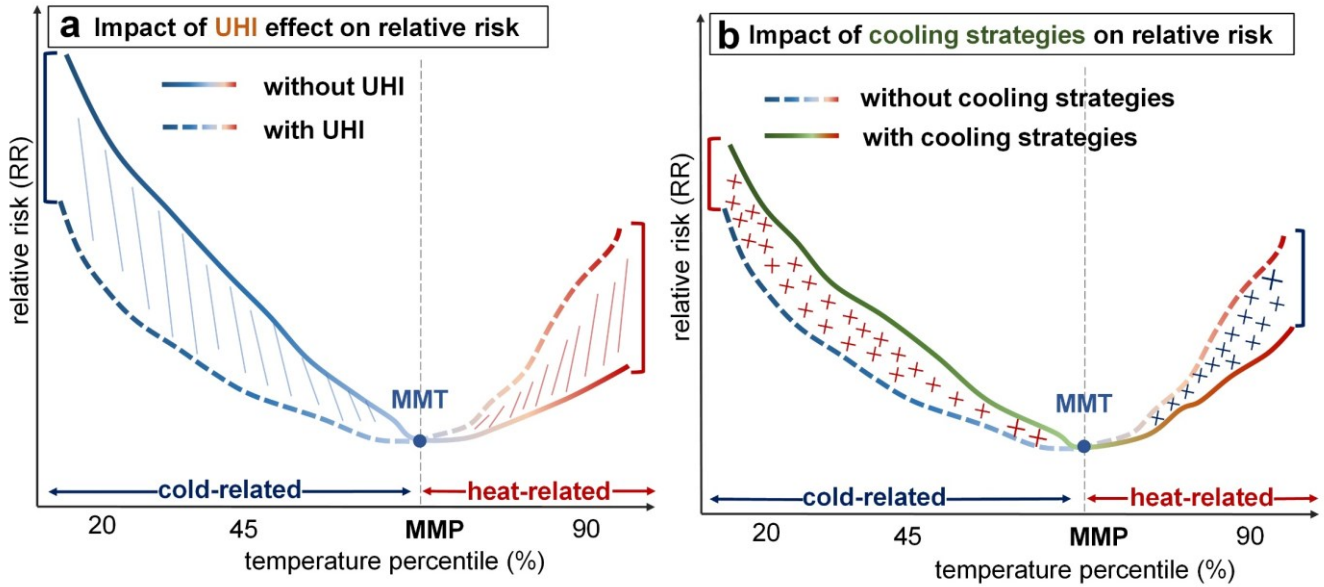
68 impacts of the UHI effect on cold- and heat-related mortality. Understanding this

69 tradeoff will facilitate the context-sensitive design of urban heat mitigation strategies

70 that modify thermal environments appropriately, given the geographic and climatic

71 settings of growing urban populations worldwide^{5, 15}.

72



73

74 **Fig. 1. The dual impacts of the UHI effect (a) and heat mitigation effects (b) on cold- and heat-**

75 **related mortality relative risk (RR) for a hypothetical city, with the annual net impact representing**

76 **the sum of the beneficial and detrimental impacts** | The two curves in **a** depict the RR variation with

77 temperature percentiles in two scenarios: without and with the UHI effect. The two curves in **b** depict

78 the RR changes with temperature percentiles in two scenarios: without (i.e., the curve with the UHI

79 effect in **a**) and with urban cooling strategies. The temperature percentile (%) represent the distribution

80 of daily air temperatures in a hypothetical city. These curves conceptualize the well-established U-

81 shaped relationship between temperature and mortality RR, identifying a minimum mortality

82 temperature (MMT, °C) and corresponding percentile (MMP, %) where RR is lowest. Above this

83 MMP/MMT, the city encounters increased heat-related RR; below it, increased cold-related RR. The

84 UHI effect typically elevates temperatures, exacerbating heat-related RR, while urban cooling strategies

85 decrease these risks. Conversely, below the MMP/MMT, the UHI effects are beneficial by moderating

86 cold temperatures, but cooling strategies may increase cold-related RR.

87 The adverse impacts of the UHI effect on urban energy use, economy, and human
88 health are well-documented in the literature^{4,13,15,17}. Conversely, several seminal
89 studies have highlighted the beneficial impacts of the UHI effect on urban
90 environments^{18,19}. However, only a handful of comprehensive studies have
91 concurrently examined both the positive and negative effects of the UHI on mortality,
92 thereby underscoring its dual nature^{15,20}. A recent pivotal study demonstrated that in
93 central Birmingham, the UHI effect could increase heat-related mortality by an
94 additional 96 cases in summer, yet it could reduce cold-related mortality by 266 cases
95 in winter, ultimately resulting in a beneficial annual net effect on mortality²¹. Further
96 critical regional studies suggest that the UHI effect may yield a beneficial annual net
97 effect on cities in higher latitudes, whereas it tends to have a detrimental annual net
98 effect on cities closer to the Equator^{22,23}, thereby indicating a regionally variable
99 impact. Cities situated in warmer regions typically exhibit a lower minimum mortality
100 percentile (MMP), which is defined as the temperature percentile corresponding to the
101 minimum mortality temperature (MMT) where the temperature-related relative risk
102 (RR) reaches its nadir. A reduced MMP implies extended exposure to heat stress for
103 inhabitants⁵. Although residents in hotter climates may develop a higher tolerance to
104 increased temperatures, the ramifications can still be significant due to sustained and
105 intense heat exposure, thereby heightening their vulnerability to the detrimental
106 impacts of the UHI effect. In contrast, cities in colder climates may derive benefits
107 from the UHI effect²¹. Theoretically, the dual impact of the UHI effect on annual
108 mortality primarily depends on the MMT (or MMP) and the shape of the mortality-
109 temperature curve²⁴ (see Fig. 1a), and is indirectly associated with the background
110 climate, as well as socioeconomic and demographic factors specific to each city²⁵.
111 Consequently, whether the net UHI-induced effects on mortality are beneficial or

112 detrimental varies considerably between cities²⁰.
113
114 Increasing vegetation and adjusting albedo are widely recognized cooling strategies
115 employed to alleviate urban heat stress²⁶⁻³¹. For example, enhancing vegetation has
116 been shown to reduce UHI-induced mortality by 39.5% in European cities³².
117 Similarly, increasing albedo can offset approximately 18.0% of UHI-induced
118 mortality in the West Midlands, United Kingdom³³. Comparable to the impacts of the
119 UHI effect, the outcomes of these cooling interventions on temperature-related
120 mortality are anticipated to be twofold: they may both decrease heat-related mortality
121 and potentially increasing cold-related mortality due to lowered urban temperatures.
122 The beneficial impacts of cooling interventions on mitigating heat risk have been
123 well-documented²⁷⁻³¹, yet their adverse impacts on cold-related mortality have been
124 less explored until recently^{21,34}. Cool roofs have been demonstrated to exacerbate
125 cold-related mortality marginally by about 0.1%, while the impacts of green roofs on
126 cold-related mortality is slightly less pronounced³⁴. Likewise, a slight exacerbation in
127 cold-related mortality was also reported due to cool roofs²¹. Theoretically, such an
128 exacerbation effect should be related to the intensity of cooling and effectiveness of
129 regulation, and therefore, should vary substantially across various urban settings.
130
131 Despite notable advancements in comprehending the dual nature of the UHI effect
132 and urban cooling strategies, several critical knowledge gaps persist. **First**, previous
133 research has explored both the beneficial and detrimental effects of the UHI effect on
134 temperature-related mortality under current and projected climate scenarios,
135 emphasizing the need to consider its dual impact, while these studies have primarily
136 focused on local or regional scales. A comprehensive global analysis remains largely

137 neglected, primarily due to the lack of precise methods necessary for obtaining UHI
138 intensity and deriving city-specific mortality-temperature correlations, particularly in
139 cities within the Global South. **Second**, the potential adverse effects of urban cooling
140 strategies on cold-related mortality, and their overall impact on annual net mortality
141 across various global cities, have not been extensively investigated, despite the broad
142 acknowledgment of their advantages. This gap in knowledge is likely exacerbated by
143 the global computational constraints of numerical simulations that are crucial for
144 assessing the efficacy of prevalent heat alleviation strategies. **Third**, the possible dual
145 impact of conventional cooling strategies on temperature-related mortality in the
146 context of global warming scenarios remains largely unexplored. It is also unclear
147 whether adaptive strategies exist that can simultaneously harness the advantages of
148 these strategies during cold seasons while minimizing their negative impact in warm
149 periods.

150

151 To address these knowledge gaps, we employed a comprehensive approach that
152 leverages multiple data sources, including remote sensing, climate, and
153 socioeconomic data. Utilizing carefully developed data-driven models with
154 computational efficiency, we established robust mortality-temperature relationships
155 and quantified the effectiveness of prevalent heat mitigation measures across more
156 than 3,000 cities worldwide. Subsequently, we scrutinized the duality of the UHI
157 effect and assessed the influence of two representative cooling strategies (increasing
158 vegetation and albedo) on temperature-related mortality on a global scale.
159 Furthermore, we projected the dual impact of these cooling interventions on future
160 mortality scenarios and proposed novel strategies to mitigate their undesired
161 consequences. Our study offers crucial guidance for formulating effective, context-

162 specific urban heat mitigation policies, thereby improving the well-being of city
163 dwellers and advancing global urban sustainability.

164 **Impacts of the UHI effect on temperature-related mortality**

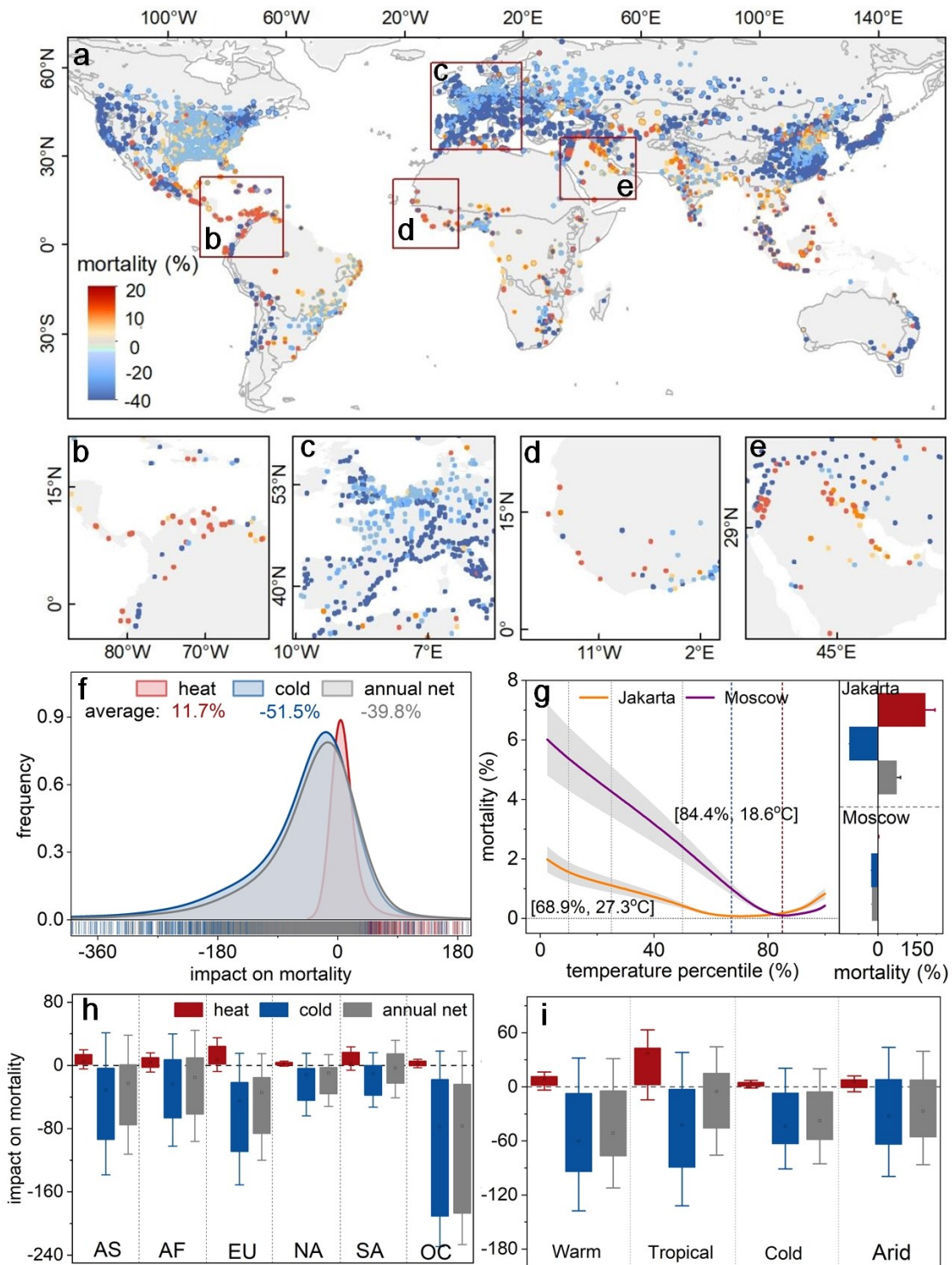
165 The dual impact of the UHI effect on annual temperature-related mortality in cities
166 exhibits global variation (Fig. 2; Supplementary Fig. S1). The reduction in cold-
167 related mortality induced by the UHI effect (51.5%; i.e., the cumulative beneficial
168 impacts in all cold days) is 4.4 times greater than the increase in heat-related mortality
169 (11.7%; i.e., the cumulative detrimental impacts in all heat days). This suggests a
170 beneficial annual net impact of the UHI effect on temperature-related mortality (Fig.
171 2f). Our analysis reveals that the global mean mortality-temperature (M-T) curve
172 shows a longer exposure period to cold temperatures than to heat, with the global
173 mean MMP reaching 77.9% (Supplementary Fig. S2). Given such a high global mean
174 MMP, the benefits induced by the UHI effect can readily outweigh the harms of
175 temperature-related mortality, resulting in a beneficial annual net effect on a global
176 scale. Even for some tropical cities (e.g., Guangzhou in China) that face significant
177 heat-related risks, the MMPs consistently remain well above 50.0% (Supplementary
178 Fig. S3). For these cities, the high-MMP effect can suppress the substantially larger
179 number of heat than cold days, leading to a beneficial annual net effect (Fig. 2a).

180

181 The annual net impacts of the UHI effect on temperature-related mortality differ
182 across climates and continents (Fig. 2a-e). Cities in high-latitude regions are more
183 exposed to cold-related risk and benefit more from the UHI effect. For instance, the
184 reduction in cold-related mortality in Moscow due to the UHI effect is 11.5 times
185 greater than the increase in heat-related mortality (Fig. 2g). In contrast, the net impact
186 of the UHI effect is predominantly detrimental for some low-latitude cities
187 characterized by high heat-related risks. For example, Jakarta in Indonesia exhibits a
188 detrimental annual net mortality effect of 72.4% (Fig. 2g). Regarding cities in

189 different climate zones, the UHI effect has a detrimental annual net effect (Fig. 2i) in
190 tropical cities (the mean MMP is 65.9%), but it is generally beneficial for other
191 climate cities, especially those in cold climate (the mean MMP is 83.8%;
192 Supplementary Fig. S4). The UHI effect has a significantly beneficial annual net
193 effect on mortality for cities in Europe and Oceania (Fig. 2h). We observe an annual
194 net positive impact over several non-tropical cities scattered across mid-to-high
195 latitudes or in arid zones (Fig. 2a). These instances are likely attributable to the
196 presence of urban cool islands over these cities (Supplementary Fig. S10), which
197 manifest in lower urban temperatures relative to the surrounding areas³⁵. Urban cool
198 islands may decrease heat-related mortality while potentially increasing cold-related
199 mortality. Furthermore, due to prolonged exposure to colder temperatures, urban cool
200 islands generally contribute to an overall annual net detrimental impact.

201



202

203

204

205

206

207

Fig. 2. Impacts of the UHI effect on cold- and heat-related mortality in global cities | Spatial

distribution of impacts of the UHI effect on annual net temperature-related mortality in cities

worldwide (a), Central America (b), Europe (c), West Africa (d), and the Middle East (e); frequency

distribution of impacts of the UHI effect on cold- related, heat-related, and annual net mortality (f;

numbers in the figure denoting the average impact); temperature-related mortality variations

208 depending on temperature percentile for Jakarta and Moscow, fitted with a B-spline function for
209 illustrative purposes (**g**), along with the UHI-induced mortality (right panel of **g**); impacts of the UHI
210 effect on cold-related, heat-related, and annual net mortality for cities by continent (**h**) and climate
211 (**i**). AF: Africa, AS: Asia, EU: Europe, NA: North America, SA: South America, OC: Oceania. The
212 impacts of the UHI effect are reflected in the cumulative values of daily temperature variations, with
213 days above the MMT defined as heat days, and those below MMT as cold days. Positive values
214 across these panels indicate an UHI-induced increase in mortality, while negative values denote a
215 reduction. Notably, some data points in panel (f) reveal that the UHI effect occasionally exacerbates
216 cold-related mortality and mitigates heat-related mortality. This phenomenon is predominantly
217 observed in cities that exhibit an urban cold island effect due to specific climatic backgrounds.
218

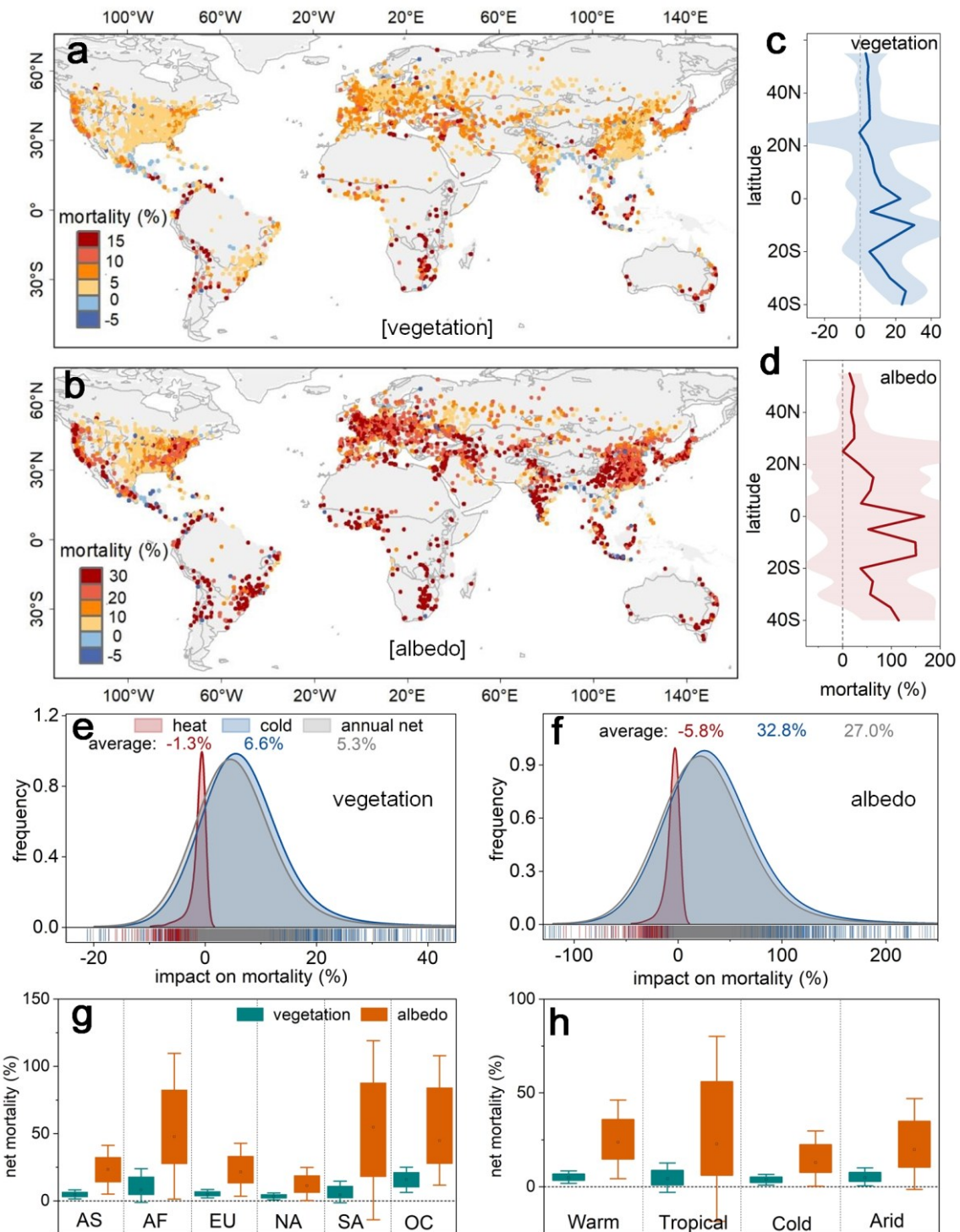
219 **Impacts of typical urban cooling strategies on temperature-related mortality**

220 We further examined the dual impacts of two commonly employed urban heat
221 mitigation strategies on temperature-related mortality in cities globally. These
222 strategies include (1) increasing the vegetation fraction by 40%, 30%, 20% of the
223 original fraction in cities with low, medium, and high population densities,
224 respectively, and (2) enhancing surface albedo by 40%, 30%, 20% of the original
225 intensity in cities with low, medium, and high albedo intensities, respectively (see
226 Methods). In line with the previous knowledge, cooling strategies such as increasing
227 vegetation fraction and surface albedo effectively reduce heat-related mortality
228 (Supplementary Fig. S5). However, these strategies can also substantially increase
229 cold-related mortality (Figs. S6 & S7). A global increase in vegetation can augment
230 cold-related mortality by 6.6% (Fig. 3e & f), a rate 5.1 times higher than the reduction
231 in heat-related mortality (Fig. 3e & f). This ratio increases to 5.6 when enhancing
232 surface albedo (Fig. 3e & f). These results suggest that these two cooling strategies
233 have a net detrimental effect on global temperature-related mortality annually.

234

235 The net impacts of these two cooling strategies on temperature-related mortality show
236 significant spatial differences across regions (Fig. 3). For cities in high-latitude
237 regions, these cooling strategies demonstrate a substantial harmful net effect on
238 annual temperature-related mortality (Fig. 3a-d). The UHI effect typically yields a
239 beneficial net effect annually for such cities (Fig. 2a), but implementing these cooling
240 strategies undermines the protective role of the UHI effect. The net impacts of these
241 cooling strategies on temperature-related mortality are minimal within the latitude
242 interval around 20°N (Fig. 3c & d). Notably, these strategies are beneficial for some
243 tropical cities, with 17.6% and 16.1% of cities benefiting for the vegetation and

244 albedo strategies, respectively. This demonstrates that the reduction in heat-related
245 mortality attributable to these cooling strategies exceeds the increase in cold-related
246 mortality. Conversely, in other climate zones, this proportion drops below 4% (Fig. 3a
247 & b). The annual net impacts of these two cooling strategies are detrimental across all
248 climate zones and continents (Fig. 3g & h). This effect is particularly pronounced in
249 cities within temperate climate, where there is a 7.7-fold increase in cold-related
250 mortality compared to the reduction in heat-related mortality for the albedo strategy
251 (Fig. 3h); and in cold climate, where the increase is 6.0 times (Fig. 3h, Figs. S6 & S7).
252 Among continents, this trend is most pronounced in cities in Oceania (22-fold) and
253 Africa (8-fold; Fig. 3g, Figs. S6 & S7).
254



255

256 **Fig. 3. Impacts of urban cooling strategies on cold- and heat-related mortality in global cities |**

257 Spatial distribution of annual net effects on temperature-related mortality with vegetation strategy (**a**)

258 and albedo strategy (**b**); changes in annual net effects depending on latitude with increasing

259 vegetation fraction (**c**) and surface albedo (**d**); frequency distribution of effects with increasing

260 vegetation fraction (**e**) and surface albedo (**f**; numbers in the figure denoting the average impact) on

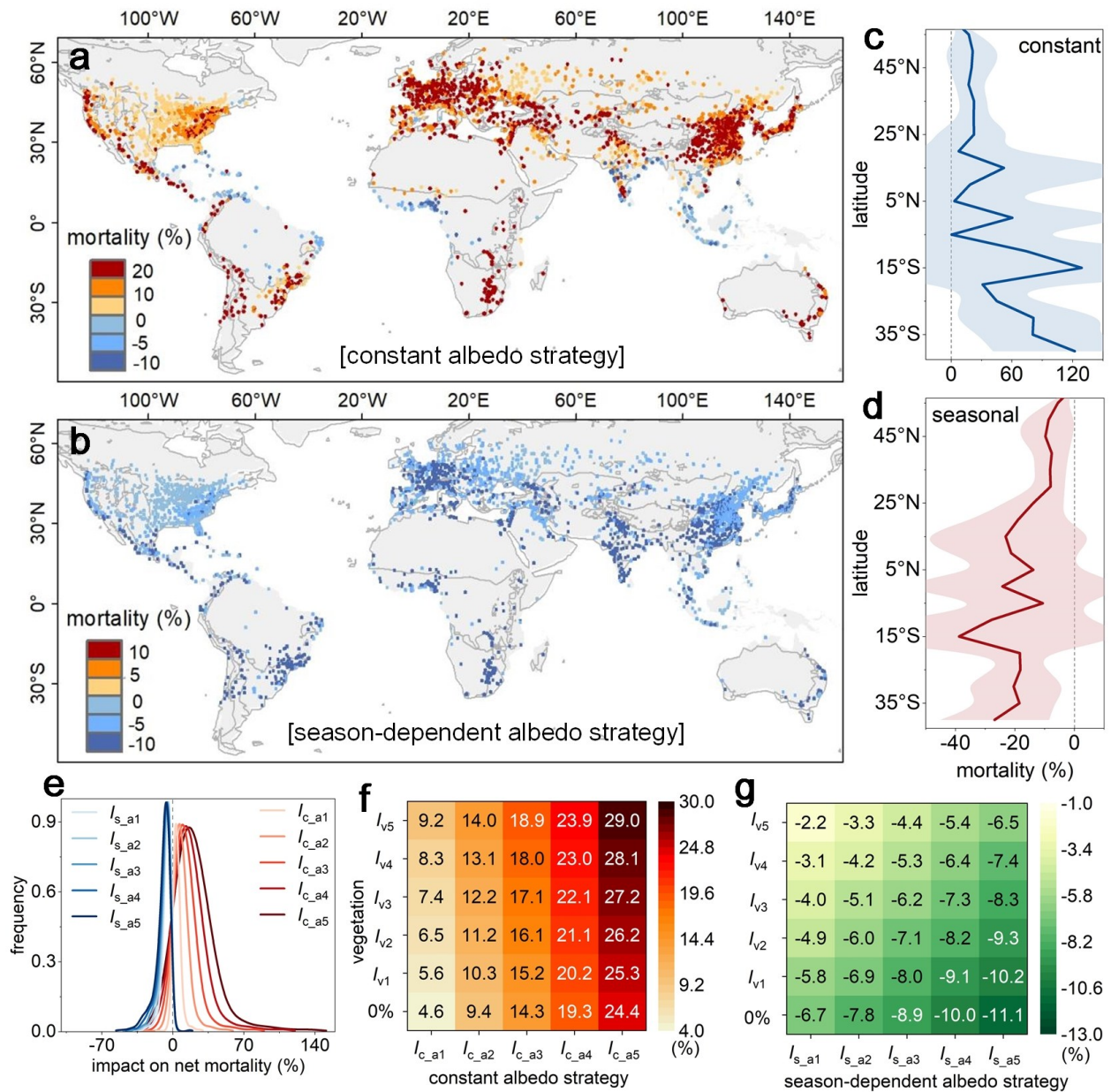
261 cold-related, heat-related, and annual net mortality; annual net effects of urban cooling strategies on
262 temperature-related mortality by continent (**g**) and climate zone (**h**). Positive values in these
263 subfigures indicate an increase in mortality due to the implementation of a specific cooling strategy,
264 while negative values indicate the opposite. AF: Africa, AS: Asia, EU: Europe, NA: North America,
265 SA: South America, and OC: Oceania.
266

267 **Impacts of cooling strategies on temperature-related mortality in the future**
268 We further analyzed the annual net impacts of several urban cooling strategies on
269 temperature-related mortality around 2050 under a moderate emission pathway
270 (SSP2-4.5; Fig. 4). The cooling strategies involve increasing urban vegetation
271 coverage and surface albedo by 4% to 40% from baseline levels, spanning five
272 regulatory intensities from low to high. These adjustments are customized for
273 different cities based on specific factors such as population density and existing
274 albedo levels (refer to Methods). Our evaluations reveal that globally, increasing
275 urban vegetation fraction could reduce future heat-related mortality by 0.2% to 1.1%
276 across the spectrum of regulatory intensities, while increasing future cold-related
277 mortality by 1.1% to 5.7% (Supplementary Fig. S8). Similarly, enhancing albedo can
278 diminish heat-related mortality by 1.1% to 5.4% but escalate cold-related mortality by
279 5.7% to 29.9% under low to high regulation intensity (Supplementary Fig. S8). We
280 observe that, by implementing these two cooling strategies, the global mean increase
281 in cold-related mortality consistently surpasses the decrease in heat-related mortality
282 (Fig. 4f). The global mean detrimental annual net impact sextuples when the cooling
283 intervention intensifies (Fig. 4f), even after factoring future global warming.
284

285 Seasonal adjustment of surface albedo (e.g., by repainting roofs and pavements) is
286 more feasible than adding vegetation over urban areas³⁰. To mitigate the adverse
287 impacts of increasing surface albedo on cold days while preserving its benefits on
288 heat days, we modified the original cooling strategy with a constant surface into a
289 season-dependent one. This season-dependent albedo strategy involves increasing
290 surface albedo on heat days, while reducing it by 8%, 6%, and 4% from baseline

291 levels on cold days for cities categorized into low, medium, and high albedo classes,
292 respectively (see Methods). This combined ‘black-white’ roof strategy is
293 engineeringly feasible, for instance, by using specific materials that change with the
294 Sun incident angle or surface temperature^{29,36,37} or through repainting roofs and
295 pavements bi-annually³⁸ (refer to Discussions and implication). Our evaluations
296 indicate that the use of a constant strategy is beneficial in most low-latitude cities
297 while detrimental in middle- and high-latitude cities in the context of future climate
298 change (Fig. 4a & c). Globally, the implementation of constant albedo and vegetation
299 cooling strategies at low regulatory intensity results in a net increase of 5.6% in
300 temperature-related mortality (Fig. 4f), which increases to 29.0 % under conditions of
301 high albedo and vegetation regulatory intensity. Nevertheless, the season-dependent
302 strategy modifies the adverse effects of the constant cooling strategy on cold-related
303 mortality, yielding annual benefits (Fig. 4b & d). As albedo regulation intensifies, this
304 season-dependent approach not only mitigates but reverses the adverse effect (Fig.
305 4e), transforming them into positive outcomes. Consequently, the overall mitigation
306 for temperature-related mortality ranges from 2.2% to 11.1% (Fig. 4g). Specifically,
307 the net mitigation increases from 2.2% to 6.5% under high vegetation regulatory
308 intensity, from 5.8% to 10.2% under low vegetation regulation, and from 6.7% to
309 11.1% with the absence of vegetation regulation (Fig. 4g).

310



311

312

313

314

315

316

317

318

319

Fig. 4. Impacts of urban cooling strategies on cold- and heat-related mortality in 2050 under SSP2-4.5 | Impacts of two urban cooling strategies (by changing surface albedo change) on the annual net mortality in global cities, i.e., the constant albedo strategy (i.e., increasing surface albedo in all year round; **a**) and the season-dependent albedo strategy (i.e., increasing surface albedo in warm season, while decreasing it in cold season; **b**); variations in future annual net mortality depending on latitude by implementing the constant (**c**) and season-dependent (**d**) albedo strategies; comparison of changes in annual net mortality using the constant and season-dependent albedo strategies with different regulation intensities (**e**); changes in annual net mortality by combining the

320 implementation of increasing vegetation fraction and surface albedo (constant albedo strategy) with
321 different regulation intensities (**f**); and **g** mirrors **f**, but for the season-dependent albedo strategy. ' I_{v1} '
322 to ' I_{v5} ' represent the regulatory intensity of the vegetation strategy, with levels ranging from low
323 (e.g., increases of 4%, 6%, 8%) to high (e.g., increases of 20%, 30%, 40%). ' I_{c-a1} ' to ' I_{c-a5} ' indicate
324 the regulatory intensity of the constant surface albedo strategy, ranging from low (e.g., increases of
325 4%, 6%, 8%) to high (e.g., increases of 20%, 30%, 40%). ' I_{s-a1} ' to ' I_{s-a5} ' denote the regulatory
326 intensity of the season-dependent albedo strategy from low to high, i.e., surface albedo was increased
327 at varying intensities during warm seasons, whereas it was decreased by 4%, 6%, 8% of the initial
328 condition for cities with high, medium, and low albedo intensity classes during cold seasons (see
329 Methods). Positive values indicate a net increase in mortality due to a cooling strategy, and negative
330 values a decrease.

331

332 **DISCUSSIONS AND IMPLICATIONS**

333 This investigation presents a comprehensive analysis of the dual impacts of the UHI
334 effect and commonly employed cooling strategies on temperature-related mortality,
335 spanning current and future scenarios across over 3,000 cities worldwide (Figs. 2 to
336 4). Our findings underscore that the conventionally-acknowledged harmful impact of
337 the UHI effect does indeed manifest as an overall detrimental influence on
338 temperature-related mortality in most low-latitude cities (such as Jakarta) and a few
339 mid-latitude cities (Fig. 2). However, a markedly larger proportion of global cities
340 (77.0%) experience a reduction in temperature-related mortality due to the UHI effect
341 (Fig. 2). Globally, UHI-induced decrease in cold-related mortality outweighs the
342 increase in heat-related mortality by approximately 4.4 times. Furthermore, the two
343 typical cooling strategies exhibit a net detrimental annual effect on global
344 temperature-related mortality. While this finding may appear surprising, it is a
345 scientifically plausible finding given that these cooling strategies disproportionately
346 exacerbate cold-related mortality compared to heat-related mortality in most cities.
347 This is due to the extended duration of cold-related risks within an annual cycle,
348 where the global mean MMP is 77.9% (Supplementary Fig. S2). Traditional views
349 often highlight the negative impacts of the UHI effect and the positive effects of
350 cooling strategies; however, our research emphasizes the dual nature of the UHI effect
351 and the associated cooling strategies on global mortality.

352

353 **Robustness and validity of UHI-induced net mortality reduction in global cities**

354 Our assessments demonstrate the feasibility of the data-driven approach employed to
355 establish mortality-temperature (M-T) relationships tailored to individual cities,
356 achieving an acceptable level of accuracy. The correlation coefficient (r) for MMT
357 reached 0.91, accompanied by a mean absolute error (MAE) of 0.97 °C, while the
358 mean r for mortality estimates at different temperature percentiles is approximately
359 0.81, generally underpinned by a MAE of 0.12 (Supplementary Note S1). Moreover,
360 our sensitivity analysis indicates that biases in the model exert only a minor influence
361 on the assessment of UHI-induced annual net mortality (Supplementary Fig. S14),
362 affirming the robustness of our study's core conclusions (Supplementary Note S3).
363 Concerns may arise among practitioners regarding the validity of extrapolating global
364 city-specific mortality-temperature (M-T) associations from a dataset with limited and
365 unevenly distributed city samples (i.e., ~700 cities; see Methods). We acknowledge
366 the inherent uncertainties associated with this approach. Nonetheless, our evaluations
367 confirm that employing the RF model alongside temperature-related data from around
368 700 cities produces reliable outcomes, despite the dataset's limited geographic
369 representation, particularly in regions of the Global South (Supplementary Note S6).
370 Another potential concern may be whether dividing the M-T association curve into
371 four distinct ranges introduces uncertainties that could potentially skew the findings.
372 Upon further analysis, we found that although some variability in the M-T association
373 might arise from this division, the four-range partitioning strategy does not
374 compromise the assessment of the dual impacts of the UHI effect on global mortality
375 (Supplementary Note S2 & Fig. S9).
376
377 Numerous investigations on M-T associations have consistently highlighted a marked
378 distinction, showing that mortality during cold seasons exceeds that during hot

379 seasons by a factor of five to twenty in most urban settings^{2,5,39}. Consequently, it is
380 anticipated that the heightened warmth attributed to the UHI effect in most cities
381 (with a relative warmth of approximately 1.0 K) would lead to a notably greater
382 reduction in cold- than in heat-related mortality. Recent observational data,
383 encompassing the past two decades and reflecting substantial warming akin to the
384 relative warmth attributed to the UHI effect, indicate a substantial prevalence of cold-
385 related over heat-related mortality³⁹. Projections concerning temperature-related
386 mortality also affirm that, even under high-emission scenarios with temperature
387 increases during both hot and cold periods, heat-related mortality is projected to
388 remain considerably lower than cold-related in most cities worldwide until 2050^{40,41}.
389 This phenomenon can be attributed to two key aspects: (1) the M-T curve displays an
390 extended tail (i.e., the MMP often exceeds 50% considerably) at lower temperature
391 percentiles, as opposed to higher percentiles, in most cities (Supplementary Fig. S2);
392 and (2) there is a notable asymmetry between the occurrence of cold and hot days,
393 particularly in mid- and high-latitude cities, with substantially more cold days
394 prevailing. Our findings underscore the imperative for clarifying the dual impact of
395 the UHI effect on annual net mortality across global cities, which holds particular
396 importance for the broader scientific community and requires further clarification.

397

398 **Added value and novelties of this study compared to previous literature**

399 Previous UHI studies have disproportionately centered on hot seasons, during which
400 UHI impacts are net negative^{8,28,42,43}. In contrast, our study investigates the dual
401 nature of the UHI effect (see Fig. 1), scrutinizing its beneficial and adverse impacts on
402 temperature-related mortality throughout an annual cycle. A few recent studies have
403 acknowledged the dual impact of the UHI effect on temperature-related mortality at a

404 city or regional scale, revealing a detrimental net annual effect, particularly evident in
405 lower-latitude cities²¹⁻²³. What sets our present investigation apart lies in its scope and
406 its delicate inputting of city-specific, context-dependent UHI intensity and
407 temperature-mortality association with satisfactory accuracy. Notably, our study focus
408 is global, involving cities in the Global South while incorporating a delicate
409 derivation of UHI intensity and M-T association through data-mining techniques (see
410 Methods).

411

412 Our study shows that the UHI effect can yield a net annual benefit even for Global
413 South cities, including those in the southern regions of Africa and South America
414 (refer to Fig. 2). In addition, we provide, to the best of our knowledge, the first
415 analysis of the impacts of two common cooling strategies on temperature-related
416 mortality across global cities. These estimates, achieved once more through a novel,
417 cost-effective data-driven approach (refer to Methods), overcome the computational
418 bottlenecks inherent in numerical simulation methods, thereby quantifying the
419 efficiency of cooling strategies for each city worldwide.

420

421 Our study distinguishes from prior research by providing evaluations of the net impact
422 of urban cooling strategies on temperature-related mortality, and by proposing
423 practical engineering solutions to mitigate the adverse effects of conventional cooling
424 methods. In contrast to previous estimations related to temperature-related mortality,
425 our research differentiates itself by incorporating variations in vulnerability due to
426 economic advancements and aging, which reshape M-T associations. We achieved
427 these predictions by establishing links between the key features of the M-T curve and
428 several climatic and socioeconomic factors, including population structure (refer to

429 Methods).

430

431 Our study involves an interdisciplinary framework. Compared to traditional urban
432 climate studies, which typically assess UHI-associated mortality using climate-level
433 temperature-relative risk (RR) curves²², our research provides a more detailed
434 interpretation of the city-specific mortality-temperature (M-T) relationship, though
435 certain uncertainties remain for some cities in the Global South where observational
436 M-T records are sparse (Supplementary Note S2). In contrast to public health studies
437 that predict future UHI intensity based on a simple exponential relationship with
438 population growth¹⁴, our approach utilizes more sophisticated and accurate methods
439 for projecting UHI intensity. Additionally, our research enhances the evaluation of
440 heat mitigation strategies by integrating robust machine learning algorithms and a
441 comprehensive set of variables. These improvements are particularly noticeable for
442 cities in the Global South, where reliable urban climate data often remains scarce or
443 absent. Exceptions are two studies by Lungman et al. (32) and Huang et al. (20), which
444 commendably bridge the gap between two disciplinary fields – urban climate and
445 public health. However, these recent endeavors limit their geographical to Europe,
446 whereas our study encompasses a broader spatial context and extends across a more
447 extensive temporal horizon by offering future projections (Figs. 2 to 4).

448

449 **Implications and caveats on the design of urban cooling strategies**

450 Our results show that the UHI effect poses a substantial adverse annual net effect on
451 mortality in most equatorial tropical cities, contrasting with an overall benefit
452 observed at the global scale (Fig. 2). UHI-induced detriments on mortality become
453 more prevalent over a considerable portion of cities in Central America (e.g., Panama

454 City), nations along the Gulf of Guinea in Africa (e.g., Douala, Cameroon), and
455 Southern South Asia (e.g., Colombo, Sri Lanka). Our findings should not undermine
456 the imperative of implementing urban heat mitigation measures in these cities to
457 address the burden of temperature-related mortality. On the contrary, the urgency of
458 implementing urban cooling strategies becomes even more pronounced for such cities
459 considering the upcoming surface warming trends⁴⁴, augmenting heat exposure due to
460 rapidly growing urban populations⁵, and their high vulnerability to heat stress⁴⁵.

461

462 Our results show a global adverse annual net impact on temperature-related mortality
463 by implementing cooling strategies (e.g., increasing vegetation fraction and surface
464 albedo; Fig. 3a & b), especially for most mid- and high-latitude cities. For these cities,
465 the conventional cooling strategies weaken the beneficial role of the UHI effect
466 during cold spells, thus amplifying cold-related mortality. These findings show that
467 typical cooling strategies fail to in attain their intended objective of reducing
468 temperature-related mortality. Our results reveal that, for such cities, the detrimental
469 impact of conventional urban cooling strategies on cold-related mortality would
470 persistently outweigh their positive effects, even under moderate global warming
471 scenarios extending until at least 2050 (Fig. 4a). Findings prompt a comprehensive re-
472 evaluation of the benefits of urban cooling strategies in the contexts of annual net
473 impacts for future applications.

474

475 Our findings, which reveal a net negative impact on mortality from increased
476 vegetation in most cities, suggest a preference for deciduous trees over evergreen
477 counterparts. Deciduous trees, reducing evaporative cooling and shade in winter by
478 shedding leaves, can minimize cold-related mortality while preserving cooling

479 benefits and other socio-ecological advantages during the summer⁴⁶. Furthermore, our
480 results indicate the viability of removable and dismountable shading shelters as an
481 effective means for curbing heat-related mortality during the summer while retaining
482 the benefits of the UHI effect in winter⁴⁷. We tested a new seasonal albedo
483 management strategy involving wintertime albedo reduction using adaptable roofing
484 materials that modify albedo in response to sun incident angles or surface
485 temperatures²⁹. This strategy aims to alleviate the negative impact on cold-related
486 mortality (Fig. 4). Although the concept of albedo reversal holds engineering
487 feasibility³⁶⁻³⁸, its citywide implementation may pose challenges due to potentially
488 high costs and amount of materials. Nevertheless, this strategy could be used at a local
489 scale, particularly over critical areas with high vulnerability, such as those densely
490 populated by elderly individuals. We must emphasize that comprehensive economic
491 assessments and life cycle analyses remain necessary at various spatial scales to
492 thoroughly analyze the cost-effectiveness of this albedo-reversal strategy¹⁶.

493

494 We need to emphasize that the observed net negative mortality impact associated with
495 increased vegetation in most mid and high-latitude cities should not be misconstrued
496 as a discouragement against incorporating green infrastructure into urban
497 development or urban renewal initiatives. Mid-latitude cities such as Shanghai, China,
498 Rome, Italy, and Phoenix, United States, exemplify instances where urban vegetation
499 is pivotal in reducing urban heat-related mortality via evaporative cooling and
500 shading⁴⁸. Urban green infrastructure facilitates surface cooling and yields
501 multifaceted co-benefits such as ecological enhancements, recreational spaces, health
502 improvements, and reduced air pollution⁴⁹. Therefore, urban green infrastructure
503 remains valuable for achieving urban sustainability. Rather than negating the value of

504 green infrastructure, our current study seeks to highlight the duality of the UHI effect,
505 wherein urban heat can function as a protective shield against cold-related mortality,
506 particularly over high-latitude cities in extreme cold events^{13,29}. Our results also
507 underline urgent actions to safeguard the public from cold temperatures, a largely
508 underserved aspect, as evidenced lucidly by our previous literature review. Similarly,
509 measures designed to mitigate urban heat during warm seasons may inadvertently
510 negatively impact on temperature-related mortality during cold seasons²⁹. The dual
511 nature of cooling strategies warrants careful consideration when introducing any new
512 heat mitigation measures.

513

514 **Possible uncertainties and concluding remarks**

515 We have demonstrated that delicate machine learning extrapolation of the M-T
516 association would not invalidate our core findings (Supplementary Note S2 & Note
517 S6). However, we must emphasize that practitioners should be cautious when
518 employing machine learning-derived M-T associations in mortality studies that
519 demand precise and sensitive M-T curve data. Furthermore, it is important to
520 underscore that machine learning approaches cannot replace the traditional collection
521 of M-T data from hospitals. This is particularly pertinent in cities within the Global
522 South, where reliable data remains limited. We acknowledge the existence of other
523 uncertainties regarding our approach, such that the vegetation type was not fully
524 considered (Supplementary Note S9). Vegetation and albedo were modified to
525 represent hypothetical heat mitigation scenarios, and the extrapolation and projection
526 of temperature-related mortality overlooked several crucial factors such as the use of
527 wet bulb temperature (Supplementary Note S8). However, it is safe to state that these
528 uncertainties would not overturn our principal findings that a prominent duality of

529 urban heat concerning temperature-related mortality exists and that urban heat can act
530 as an effective shield to reduce cold-related mortality, especially for non-tropical
531 cities. We also acknowledge that our estimates assume continuous outdoor urban heat
532 exposure (Supplementary Note S7), a methodological choice consistent with most
533 previous epidemiological studies. With individuals spending increased time indoors,
534 indoor temperature management has an even more significant impact on heat stress.
535 In this context, the cost-benefit analysis shifts towards considerations of energy
536 demand implications rather than mortality, a realm where the UHI effect has been
537 evidenced to have a net reduction in energy demand for colder cities²².

538

539 Our analysis implies that, within a moderate emission trajectory, the UHI effect is
540 poised to yield more detriments than benefits regarding temperature-related mortality
541 around 2050 for most mid-latitude cities (Fig. 4). However, projections suggest that
542 the increase in heat-related mortality instigated by the UHI effect should outweigh the
543 decrease in cold-related mortality across cities in Central and Southern Europe and
544 South America during the latter half this century⁴⁰. It is important to note that our
545 current estimates are grounded in temperature-mortality curves derived primarily
546 from mortality data collected in the early years, around 2000⁵. This raises the concern
547 that the mortality data from this period may no longer reflect current climatic
548 conditions, particularly for cities that have witnessed an increase in extreme heat
549 events, such as Phoenix and Los Angeles in the United States⁵⁰. Furthermore, our
550 estimates do not consider the substantial and abrupt surge in heat-related mortality
551 arising from extreme heat events⁵¹, which are expected to gain prominence under
552 global warming scenarios⁵². In this changing climate landscape, the UHI effect in
553 many mid-latitude cities might yield an annual net adverse impact even significantly

554 before 2050 under low or moderate emission pathways. Finally, our study seeks to
555 further communicate several critical points by illustrating the global duality of urban
556 heat on mortality: (1) protecting urban dwellers from the cold is equally, if not more,
557 critical as protecting them from heat; (2) seasonally adjustable strategies are critical to
558 cool and warm urban surfaces on heat and cold periods respectively, but economic
559 viability is of great importance; and (3) urban policy-makers need to consider the
560 escalating heat-related mortality associated with global warming scenarios when
561 designing adaptation measures, as relevant time scales for city adaptation under
562 climate change span decades rather than years.

563

564

565 **METHODS**

566 **Study area and data**

567 We chose 3,280 cities worldwide, each with an urban area exceeding 30 km² in
568 2018⁵³, to investigate the impacts of the UHI effect and urban cooling strategies on
569 annual net temperature-related mortality. These cities span across Asia (1394 cities),
570 Europe (614 cities), North America (841 cities), South America (188 cities), Africa
571 (196 cities), and Oceania (47 cities). Additionally, employing the Köppen-Geiger
572 climate zone⁵⁴, we classified these cities into equatorial (441 cities), arid (379 cities),
573 warm (1706 cities), and snow cities (754 cities).

574

575 The data used include mortality-temperature (M-T) data, Moderate Resolution
576 Imaging Spectroradiometer (MODIS) data, satellite-based urban surface air
577 temperature (SAT) data, climate data, socioeconomic data, and other ancillary data.

578 The city-specific M-T associations were obtained from Gasparrini et al. (5) and
579 Kephart et al. (2). These results were derived from official mortality records from
580 approximately 700 cities worldwide (Supplementary Fig. S11), meticulously
581 documenting location-specific mortality variations at various temperature percentiles
582 ranges (e.g., 5%, 10%, 90%, and 95%). The M-T data were utilized to assess the
583 impacts of the UHI effect and associated urban cooling strategies on temperature-
584 related mortality.

585

586 The MODIS data consist of the 16-day enhanced vegetation index (EVI; product
587 name: MOD13Q1; 250 m spatial resolution) and the daily albedo estimates
588 (MCD43A3; 500 m). We employed the 2017-2018 EVI and albedo data to portray the
589 spatial distribution of urban vegetation and albedo in cities worldwide and to assess

590 the impact of urban cooling strategies achieved through increasing the vegetation
591 fraction and surface albedo on temperature-related mortality.

592

593 The urban SAT data were obtained from the global near-surface air temperature
594 dataset (1 km spatial resolution) generated based on a series of satellite-derived
595 surface variables and *in-situ* SATs obtained from over 100,000 stations⁵⁵. The
596 generated SATs offer a reliable depiction of surface air temperature spatiotemporal
597 patterns. Cross-validations have demonstrated that the generated SATs are highly
598 accurate (with a mean absolute error of 1.49 °C), particularly over impervious
599 surfaces⁵⁵. This dataset enhances the capture of spatial variations in biophysical and
600 socioeconomic factors affecting temperature⁵⁵, thereby facilitating an accurate
601 quantification of the urban heat island (UHI) effect. The dataset's accuracy should be
602 adequate for our purposes, as it achieves a level of precision comparable to existing
603 products⁵⁵. Furthermore, we employ this dataset to compute UHI intensity, defined as
604 the difference between the mean urban temperature and the mean suburban
605 temperature, rather than absolute temperature values. This subtraction could
606 effectively reduce bias associated with absolute temperature measurements⁹². To
607 derive daily mean values, we average the daily maximum and minimum surface air
608 temperatures (SAT). The mean SAT was used to quantify the canopy-layer UHI
609 intensity, aligning with the daily mean temperature in the M-T associations.

610

611 Our data were obtained from the ERA5-Daily and monthly ERA5-Land reanalysis
612 datasets and the Coupled Model Intercomparison Project Phase 6 (CMIP6)
613 dataset^{56,57}. From the ERA5-Daily reanalysis dataset (9 km spatial resolution)⁵⁸, we
614 retrieved the daily mean SAT at 2-m height above ground to represent the daily

615 background air temperature. We retrieved the precipitation, wind speed, and radiation
616 data for each city from the monthly ERA5-Land reanalysis dataset. These three
617 climate variables served as background climate inputs for calibrating the impact of
618 urban cooling strategies on urban temperatures. Additionally, from the CMIP6
619 dataset^{56,57}, we retrieved the daily surface air temperature, relative humidity, and
620 precipitation in 2050 under a moderate emissions pathway (SSP2-4.5). These data
621 were considered as background climate factors for estimating future UHI intensity.
622

623 The socioeconomic data encompass Gross Domestic Product (GDP), the Critical
624 Infrastructure Spatial Index (CISI), the Human Development Index (HDI), and
625 population data. GDP data (2017 to 2018) were extracted from the global long-term
626 GDP dataset (1 km spatial resolution) generated based on improved nighttime light
627 data⁵⁹. The CISI, with a spatial resolution of 0.1°, quantifies the spatial intensity of
628 urban infrastructure globally, utilizing high-resolution geospatial data from Open
629 Street Map (OSM) for 39 types of critical infrastructure⁸⁹, such as hospitals. The HDI
630 is a composite index that captures essential aspects of human development—health
631 and longevity, knowledge, and standard of living—derived from a global time-series
632 product with a spatial resolution of 5 arc-minutes⁹⁰. These indices, along with GDP
633 data, were employed as predictor variables to statistically determine the M-T
634 relationship for each city worldwide. Historical (2017 to 2018) and future (2050)
635 population data were obtained from the Oak Ridge National Laboratory's LandScan
636 population dataset (<https://landscan.ornl.gov/>)⁶⁰ and the projected global population
637 dataset⁶¹, both at a spatial resolution of 1 km. The population data were used to
638 calculate the urban population for each city. Furthermore, population data for different
639 age groups in various countries and territories were obtained from the United Nations¹

640 to gather population structure information. This information was then assigned to
641 cities within each territory to quantify the proportion of the population aged over 65.
642 The assigned proportion was used as an age structure factor for statistically
643 establishing the M-T relationship⁶².

644

645 The auxiliary data include the global urban boundary (GUB), elevation, and land
646 cover type data. We used the 2018 GUB data⁵³ to delineate urban and rural areas to
647 calculate the UHI intensity. The elevation data were derived from the GTOPO30
648 dataset (1 km) provided by the U.S. Geological Survey's Center for Earth Resources
649 Observation and Science (<http://lpdaac.usgs.gov>)⁶³. The elevation data were used as a
650 topographic factor in deriving the statistical M-T relationship and were used to assess
651 the impacts of cooling strategies on urban temperatures. The land cover type data
652 were sourced from the MODIS MCD12Q1 product (500 m spatial resolution). They
653 were used to remove pixels labeled as water bodies, snow and ice, and permanent
654 wetlands⁶⁴ to reduce uncertainties in calculating UHI intensity.

655

656 **Assessing impacts of the UHI effect on temperature-related mortality**

657 The M-T profile typically follows a 'U-shape' curve⁶⁵⁻⁶⁸. In such scenarios, the UHI
658 effect exacerbates heat-related mortality on hot days while reducing cold-related
659 mortality on cold days (Fig. 1). Our assessment of the UHI-induced annual net impact
660 on temperature-related mortality complied with the following three steps. First, we
661 calculated the SAT-based UHI intensity for global cities. Second, we estimated the
662 parameters of the M-T (daily mean temperature for this study) curve for each city.
663 Third, we comprehensively assessed the annual net impact of the UHI effect on
664 temperature-related mortality in cities worldwide. A complete flowchart for assessing

665 the UHI impacts on temperature-related mortality is provided in Supplementary Fig.
666 S12.

667

668 **(1) Calculating SAT-based UHI intensity for global cities**

669 The urban heat island (UHI) effect, a distinct local climate phenomenon, manifests as
670 greater temperatures in urban areas compared to suburban areas due to urbanization⁶.
671 Conversely, a minority of cities exhibit an urban cold island effect, primarily in arid
672 climates⁸⁸. The common approach to measuring this effect involves calculating the
673 temperature difference between the average temperatures of urban and suburban
674 area⁷¹. In our study, urban surfaces were delineated using urban areas identified from
675 the 2018 GUB data, while rural surfaces were defined as the areas within the 10-km to
676 50-km buffers surrounding the urban areas⁶⁹. To minimize uncertainties associated
677 with specific land cover types like 'ice', 'snow', 'water', and 'permanent wetland',
678 corresponding pixels were excluded from urban and rural surfaces when calculating
679 UHI intensity⁷⁰. We then computed the UHI intensity (UHII) as the average surface
680 air temperature (SAT) difference between these defined urban and rural surfaces. This
681 UHII was determined on a monthly basis for global cities (Supplementary Fig. S10).

682

683 **(2) Quantifying the mortality-temperature association for each city worldwide**

684 Previous studies indicate that the mortality-temperature association is best quantified
685 by considering temperature percentile rather than absolute temperature^{72,73}. Two
686 distinct features characterize this association: the minimum mortality temperature
687 (MMT) and the 'U-shaped' M-T curve. MMT represents the optimum temperature at
688 which the minimum mortality occurs, while the minimum mortality percentile (MMP)
689 denotes the percentile of MMT (Fig. 1). Urban populations face heat-related mortality

690 risks when the daily temperature exceeds MMT. At the same time, cold-related
691 mortality risks arise when the daily temperature is lower than MMT⁶⁵. The values of
692 MMT and the 'U-shaped' M-T curve differ depending on the cities' background
693 climate and socioeconomic conditions²⁵. Obtaining information on MMT and the 'U-
694 shaped' M-T curve can often be challenging, if impossible, especially for most cities
695 in developing and underdeveloped nations. This is primarily due to the heavy reliance
696 on comprehensive and detailed official mortality records documented in hospitals and
697 medical centers to ascertain MMT and the 'U-shaped' M-T curve.

698

699 We developed a machine learning method to acquire each city's MMT and 'U-shaped'
700 data using M-T information from a constrained set of cities⁷⁴. Our investigation
701 sourced comprehensive M-T curves from approximately 700 cities worldwide,
702 meticulously extracted from official mortality records^{2,5}. This set of cities
703 encapsulates diverse background climates and socioeconomic contexts by
704 encompassing nineteen nations (Supplementary Fig. S11), including the USA,
705 Canada, UK, Italy, Spain, Sweden, China, Japan, South Korea, Thailand, Australia,
706 Brazil, Argentina, Chile, Mexico, Peru, Costa Rica, El Salvador, and Guatemala. This
707 set of cities offers intricate data concerning MMT and the 'U-shape' at different
708 temperature percentiles (e.g., 5%, 10%, 50%, 90%, and 95%). We uniformly
709 integrated these mortality percentiles into four categories (i.e., >5%, 5%-MMT,
710 MMT-95%, and >95%), representing mortality variations from extreme cold, non-
711 extreme cold, non-extreme heat, to extreme heat, respectively. We trained a random
712 forest (RF) model to establish a statistical relationship between dependent variables
713 (i.e., the MMT and mortality at four percentiles) and a range of climatic,
714 socioeconomic, and urban infrastructure factors. These factors encompassed SAT,

715 dew point temperature, precipitation, wind speed, altitude, and latitude/longitude,
716 GDP, population structure (the proportion of population aged over 65)⁶², CISI, and
717 HDI. The rationale for selecting these indicators is elaborated in Supplementary Note
718 S4. The RF model was trained using data from the above-noted cities and then applied
719 to infer the MMT (Supplementary Fig. S3) and mortality at different temperature
720 percentiles for over 3,000 cities worldwide. Additionally, we estimated the MMPs
721 using a similar approach to illustrate the relationship between mortality and
722 temperature percentile (Supplementary Fig. S3). This characterization is intended to
723 facilitate an intuitive understanding of the discrepancies in temperature-related
724 mortality across cities.

725

726 On this basis, we utilized global daily air temperature data to quantify temperature
727 intensity values across various temperature percentiles for each city. By referencing
728 the established U- or V-shaped temperature-mortality relationship^{2,65,73}, we derived
729 the specific correlations between temperature and mortality within each temperature
730 percentile interval. This derivation enables us to quantify the increase in heat-related
731 mortality or the decrease in cold-related mortality for each 1°C rise in temperature².
732 By employing this relationship along with daily air temperature data from cities
733 worldwide, we estimated the daily temperature-related mortality for each city under
734 any given day of temperature conditions. By accumulating daily mortality and
735 categorizing days with temperatures above the MMT as heat days and below as cold
736 days, we then calculated the city-specific cold-related and heat-related mortality. The
737 detailed calculation procedures are provided in Supplementary Fig. S13.

738

739 **(3) Assessing the impact of the UHI effect on annual net mortality for each city**

740 To examine the impact of the UHI effect on cold-related and heat-related mortality,
 741 we first categorized the cold and warm months for each city based on global MMT
 742 estimates (Supplementary Fig. S3). Months during which temperatures exceeded the
 743 MMT were classified as warm, while those with temperatures below the MMT were
 744 categorized as cold. We then calculated the UHI values for the cold and warm seasons
 745 by averaging the UHI intensity across the respective months. Based on the
 746 temperature-mortality relationship (i.e., increased heat-related mortality or decreased
 747 cold-related mortality per 1 °C increase in temperature), we quantified the
 748 temperature-related mortality by simultaneously considering background temperature
 749 and UHI. The impact of the UHI effect on temperature-related mortality was
 750 subsequently isolated by comparing the difference in temperature-related mortality
 751 with and without considering the UHI effect, using the following equation:

$$752 \quad \begin{cases} M_{\text{heat_UHI}} = \sum_{T_a}^{T_a} (M_{T_a_UHI_{\text{heat}}} - M_{T_a}) \\ M_{\text{cold_UHI}} = \sum_{T_a}^{T_a} (M_{T_a_UHI_{\text{cold}}} - M_{T_a}) \end{cases} \quad (2)$$

753 where T_a represents the daily mean temperature; ' mmt ' denotes the minimum mortality
 754 temperature; UHI_{heat} and UHI_{cold} denote the UHI intensity values for the cold and
 755 warm seasons; $M_{T_a_UHI_{\text{heat}}}$ and $M_{T_a_UHI_{\text{cold}}}$ represent the heat- and cold-related
 756 mortality with the UHI effect; M_{T_a} represent the temperature-related mortality without
 757 the UHI effect; and $M_{\text{heat_UHI}}$ and $M_{\text{cold_UHI}}$ denote the additional impacts of the UHI
 758 effect on heat- and cold-related mortality, respectively. The UHI-induced annual net
 759 impact encompassing both heat and cold-related mortality is calculated as follows:

$$760 \quad M_{\text{net_UHI}} = M_{\text{heat_UHI}} + M_{\text{cold_UHI}} \quad (3)$$

761 where $M_{\text{net_UHI}}$ denotes the UHI-induced annual net impact on mortality (unit: %).
 762 Positive values of $M_{\text{heat_UHI}}$, $M_{\text{cold_UHI}}$, and $M_{\text{net_UHI}}$ indicate an increase in mortality
 763 attributable to the UHI effect, while negative values suggest the opposite. $M_{\text{net_UHI}}$ is

764 the sum of UHI-increased heat-related mortality (usually positive, in percentage) and
765 UHI-reduced cold-related mortality (usually negative, in percentage).

766

767 **Assessing effects of urban cooling strategies on temperature-related mortality**

768 We investigated the effects of two common urban cooling strategies: increasing
769 vegetation and changing surface albedo. We examined temperature-related mortality
770 in cities worldwide for the present (for the year 2018) and future (for the year 2050).
771 First, we quantified the cooling effects of specific vegetation and albedo changes by
772 analyzing their relationships with urban temperatures. Next, we assessed the annual
773 net impacts of these cooling strategies on mortality for the present and future under a
774 moderate emissions pathway (SSP2-4.5). The detailed procedures followed for
775 evaluating the impacts of urban cooling strategies on temperature-related mortality are
776 provided in Supplementary Fig. S13.

777

778 **(1) Evaluating impacts of urban cooling strategies on temperature-related** 779 **mortality for the present**

780 The efficacy of cooling strategies, such as increasing vegetation fraction and surface
781 albedo, in mitigating urban temperatures can typically be assessed using numerical
782 models like the Weather Research & Forecasting Model (WRF)⁷⁵⁻⁷⁷. However,
783 applying such models comprehensively to over 3,000 cities worldwide presents
784 significant challenges. Studies at global or regional scales often rely on remote
785 sensing data combined with linear regression models to evaluate the cooling
786 impacts^{32,36,91}. Establishing a linear relationship between temperature and vegetation
787 through these models facilitates a statistical analysis of how changes in vegetation
788 correlate with temperature variations.

789
790 Here, we applied a similar statistical method to evaluate the efficiency of cooling
791 strategies for over 3,000 cities worldwide, following three steps. First, to account for
792 temporal variations in vegetation/albedo, we analyzed the monthly linear relationships
793 between urban temperature and vegetation/albedo for each city, separately obtaining
794 monthly values for the fitted slopes. The slopes between urban temperature and
795 vegetation/albedo were used to determine the temperature variations due to changes in
796 vegetation and albedo^{32,78}. Second, we removed any anomalous slope values³² that
797 could be attributed to statistical instability or insignificance, often due to inadequate
798 pixel data in certain cities. Finally, we utilized a random forest algorithm to establish a
799 correction between the remaining slope values and various climatic and
800 socioeconomic factors for both cold and warm seasons. Comprehensive details on the
801 analytical process and the accuracy of the correction model are documented in
802 Supplementary Note S5. This step allows us to determine the cooling or heating
803 efficiency of vegetation and albedo changes by enhancing statistical stability across
804 cities globally. The variables incorporated in the correction process include SAT, dew
805 point temperature, precipitation, wind speed, radiation, average vegetation cover
806 (EVI), albedo, urban population, altitude, and latitude/longitude⁷⁹. A comprehensive
807 explanation of the selection of these indicators is provided in Supplementary Note S4.
808
809 Drawing from similar previous studies^{81,82}, we considered the use of percentage
810 increases in vegetation and albedo as an urban cooling strategy. The monthly
811 vegetation and albedo data were averaged to obtain the results for both cold and warm
812 seasons for global cities, and then a percentage increase was applied to the original
813 intensity in the cold and warm seasons. To accurately reflect the varying vegetation

814 growth potentials in urban environments with different population density, we first
815 classified global cities by population density percentile into three categories: 0% –
816 25% (low population density), 25% – 75% (medium population density), and 75% –
817 100% (high population density). Cities with high urban population density generally
818 have lower potential for vegetation increase, and vice versa. Therefore, we applied
819 increase percentages of 40%, 30%, and 20% as three tiers of vegetation regulation
820 strategies^{32,81,82} for these three categories, respectively. Similarly, for the albedo
821 strategy, global cities were classified into 0% – 25% (low intensity), 25% – 75%
822 (medium intensity), and 75% – 100% (high intensity) classes based on albedo
823 intensity percentiles, and an increase of 40%, 30%, and 20% was applied as the
824 albedo regulation strategy for these three classes, respectively. Subsequently, we
825 evaluated the urban cooling (UC) effects of these two strategies for individual cities
826 (Supplementary Fig. S5). Similar to Equations 2 & 3, the annual net mortality impacts
827 (M_{net_UC}) attributable to increased vegetation or albedo were calculated by comparing
828 mortality estimates with and without considering the cooling effects of these two
829 strategies, using the following equation:

$$830 \quad \begin{cases} M_{heat_UC} = \sum_{mmt}^{T_a} (M_{T_a_UHI_{heat_UC}} - M_{T_a_UHI_{heat}}) \\ M_{cold_UC} = \sum_{mmt}^{T_a} (M_{T_a_UHI_{cold_UC}} - M_{T_a_UHI_{cold}}) \\ M_{net_UC} = M_{heat_UC} + M_{cold_UC} \end{cases} \quad (4)$$

831 where M_{heat_UC} , M_{cold_UC} , and M_{net_UC} denote the impacts of the implemented cooling
832 strategies on heat-related, cold-related, and annual net mortality, with a positive value
833 indicating increased mortality associated with the cooling strategy and a negative
834 value indicating the opposite; $M_{Ta_UHI_{heat_UC}}$ and $M_{Ta_UHI_{heat}}$ represent the estimated
835 heat-related mortality with and without consideration of the cooling effects,

836 respectively; and $M_{Ta_UHIcold_UC}$ and $M_{Ta_UHIcold}$ refer to the estimated cold-related
837 mortality with and without consideration of the cooling effects, respectively.

838

839 **(2) Evaluating impacts of urban cooling strategies on temperature-related**
840 **mortality for the future**

841 The key to evaluating the impacts of cooling strategies in the future lies in estimating
842 future urban temperatures. To address this, we follow three steps. First, we trained a
843 random forest model to estimate UHI intensity based on a series of previously
844 confirmed regulators including SAT, humidity, precipitation, population, and
845 latitude/longitude⁸³⁻⁸⁵(Supplementary Note S4). Our model, validated with a randomly
846 split 30%-test dataset, demonstrated robust accuracy with a mean correlation of 0.93
847 and mean MAE of 0.18 °C (Supplementary Fig. S15). Second, with the well-validated
848 model, we projected future UHI intensity (~2050) for each city based on the
849 abovementioned predictors (Supplementary Fig. S16). Finally, we estimated future
850 urban temperature by combining the projected future UHI intensity with the
851 background temperature.

852

853 We designed five scenarios for vegetation and albedo strategies, varying from mild to
854 extreme controls, to evaluate their impacts on future mortality^{86,87}. Specifically, we
855 established intervals of 8%, 6%, and 4% for cities with low (ranging from 8% to
856 40%), medium (ranging from 6% to 30%), and high (ranging from 4% to 20%)
857 population density and albedo intensity classes, respectively, to assess the associated
858 impacts from low to high vegetation and albedo regulation. Notably, compared with
859 vegetation coverage, surface albedo offers higher adjustability throughout different
860 seasons in a year³⁰. For example, this seasonal adjustability can be achieved by

861 choosing roofs with an albedo that changes with sun angle, by using roofs with
862 thermochromic materials^{29,36,37}, or by repainting roofs and pavements³⁸. Therefore, we
863 modified the initial cooling strategy, which used fixed albedo values, into a more
864 flexible strategy that mitigates the negative impact of high albedo during cold days.
865 Note that this combined albedo strategy is engineeringly practicable^{29,36-38}, at least
866 over crucial areas of high vulnerability at the local scale. In this modified strategy,
867 surface albedo was increased with different intensities during warm seasons, while it
868 was decreased by 8%, 6%, and 4% of the initial condition for cities with low,
869 medium, and high albedo intensity classes during cold seasons. We subsequently
870 quantified the cooling effects of these control strategies (Supplementary Fig. S17) and
871 examined their annual net impacts on future mortality using Equation 4.

872

873 For these hypothetical heat mitigation scenarios, we quantified the impacts of the UHI
874 effect and the associated cooling strategies on cold-related, heat-related, and overall
875 annual net mortality in the examined 3,000-plus cities worldwide. We conducted a
876 comprehensive analysis at regional and individual city scales. The averaged impacts
877 of the UHI effect and cooling strategies at global, climate-zone, and continental scales
878 were revealed separately (Figs. 2 to 4). We acknowledge uncertainties in the analysis,
879 such as the omission of vegetation type and distinct weather conditions (e.g.,
880 snowfall). Additionally, the M-T association might change in the future. Nevertheless,
881 these uncertainties would not undermine our key findings, even if some of the
882 magnitudes of the effects are shifted. Further deliberation on these uncertainties can
883 be found in Supplementary Note S3.

884 **DATA AVAILABILITY**

885 All the satellite and reanalysis data used in this study can be downloaded on the
886 Google Earth Engine (GEE) platform ([https://developers.google.cn/earth-](https://developers.google.cn/earth-engine/datasets/catalog/)
887 [engine/datasets/catalog/](https://developers.google.cn/earth-engine/datasets/catalog/)). Global climate simulations for future periods are available
888 at <https://esgf-node.llnl.gov/search/cmip6/>. The global 1 km near-surface air
889 temperature dataset are available at <https://doi.org/10.25380/iastate.c.6005185.v1>. The
890 Gross Domestic Product (GDP) and population data are available at
891 <https://doi.org/10.6084/m9.figshare.17004523.v1> and <https://landscan.ornl.gov/>,
892 respectively. The global urban boundary dataset is available at
893 <http://data.ess.tsinghua.edu.cn/>.

894

895 **ACKNOWLEDGEMENTS**

896 We gratefully acknowledge the following organizations for providing support for this
897 current study. They include the National Natural Science Foundation of China (no.
898 42171306). We also thank the support from the National Youth Talent Support
899 Program of China. Pacific Northwest National Laboratory is operated for the
900 Department of Energy by Battelle Memorial Institute under contract DE-AC05-
901 76RL01830. We would also like to thank Prof. Josiah L. Kephart from Drexel
902 University for valuable discussions and insights.

903

904 **AUTHOR CONTRIBUTIONS**

905 W.Z. designed research; S.W. and W.Z. performed data analysis and wrote
906 manuscript; and B.Z., S.T., T.C., Z.W., K.H., H.D., A.M., J.L., Z.L., L.L., F.H., and
907 M.L. contributed ideas to data analysis, interpretation of results, or manuscript
908 revisions.

909 **COMPETING INTERESTS**

910 The authors declare no competing interests.

911

912 **REFERENCES**

- 913 1. United Nations, Department of Economic and Social Affairs, Population Division
914 2022. World Population Prospects: The 2022 Revision.
- 915 2. Kephart, J. L. et al. City-level impact of extreme temperatures and mortality in
916 Latin America. *Nat. Med.* **28**, 1700–1705 (2022).
- 917 3. Santamouris, M., Cartalis, C., Synnefa, A. & Kolokotsa, D. On the impact of
918 urban heat island and global warming on the power demand and electricity
919 consumption of buildings—A review. *Energ. Buildings* **98**, 119–124 (2015).
- 920 4. Tong, S., Prior, J., McGregor, G., Shi, X. & Kinney P. Urban heat: an increasing
921 threat to global health. *BMJ* **375** (2021).
- 922 5. Gasparrini, A. et al. Mortality risk attributable to high and low ambient
923 temperature: a multicountry observational study. *The Lancet* **386**, 369–375
924 (2015).
- 925 6. Oke, T. R. The energetic basis of the urban heat island. *Q. J. Roy. Meteor. Soc.*
926 **108**, 1–24 (1982).
- 927 7. Burnside, W. R. et al. Human macroecology: Linking pattern and process in big-
928 picture human ecology. *Biol. Rev.* **87**, 194–208 (2012).
- 929 8. Laaidi, K. et al. The impact of heat islands on mortality in Paris during the
930 August 2003 heat wave. *Environ. Health Persp.* **120**, 254–259 (2012).
- 931 9. Smargiassi, A. et al. Variation of daily warm season mortality as a function of
932 micro-urban heat islands. *J. Epidemiol. Commun. H.* **63**, 659–664 (2009).
- 933 10. Aghamohammadi, N., Ramakreshnan, L., Fong S. C. & Kumar, P. A global
934 synthesis of heat-related mortality in overheated cities. In urban overheating: heat
935 mitigation and the impact on health. *Singapore: Springer Nature Singapore*
936 (2022).

-
- 937 11. Davies, M., Steadman, P. & Oreszczyn, T. Strategies for the modification of the
938 urban climate and the consequent impact on building energy use. *Energy Policy*
939 **36**, 4548–4551 (2008).
- 940 12. Chakraborty, T., Hsu, A., Manya, D. & Sheriff, G. A spatially explicit surface
941 urban heat island database for the United States: Characterization, uncertainties,
942 and possible applications. *ISPRS J. Photogramm.* **168**, 74–88 (2020).
- 943 13. Macintyre, H. L., Heaviside, C., Cai, X. & Phalkey, R. The winter urban heat
944 island: Impacts on cold-related mortality in a highly urbanized European region
945 for present and future climate. *Environ. Int.* **154**, 106530 (2021).
- 946 14. Zhu, D., Zhou, Q., Liu, M. & Bi, J. Non-optimum temperature-related mortality
947 burden in China: Addressing the dual influences of climate change and urban heat
948 islands. *Sci. Total Environ.* **782**, 146760 (2021).
- 949 15. Heaviside, C., Macintyre, H. & Vardoulakis, S. The urban heat island:
950 implications for health in a changing environment. *Curr. Env. Hlth. Rep.* **4**, 296–
951 305 (2017).
- 952 16. Estrada, F., Botzen, W. W. & Tol, R. S. A global economic assessment of city
953 policies to reduce climate change impacts. *Nat. Climate change* **7**, 403–406
954 (2017).
- 955 17. Li, X. et al. Urban heat island impacts on building energy consumption: A review
956 of approaches and findings. *Energy* **174**, 407–419 (2019).
- 957 18. Hirano, Y. & Fujita, T. Evaluation of the impact of the urban heat island on
958 residential and commercial energy consumption in Tokyo. *Energy* **37**, 371–383
959 (2012).
- 960 19. Kolokotroni, M., Zhang, Y. & Watkins, R. The London heat island and building
961 cooling design. *Sol. Energy* **81**, 102–110 (2007).

-
- 962 20. Huang, W. T. K. et al. Assessing the impact of urban heat islands on the risks and
963 costs of temperature-related mortality (No. EGU23-9892). Copernicus Meetings
964 (2023).
- 965 21. Macintyre, H. L., Heaviside, C., Cai, X. & Phalkey, R. Comparing temperature-
966 related mortality impacts of cool roofs in winter and summer in a highly
967 urbanized European region for present and future climate. *Environ. Int.* **154**,
968 106606 (2021).
- 969 22. Fan, Y. et al. Urban heat island reduces annual building energy consumption and
970 temperature related mortality in severe cold region of China. *Urban Clim.* **45**,
971 101262 (2022).
- 972 23. Lowe, S. A. An energy and mortality impact assessment of the urban heat island
973 in the US. *Environ. Impact Asses.* **56**, 139–144 (2016).
- 974 24. Patz, J. A., Engelberg, D. & Last, J. The effects of changing weather on public
975 health. *Annu. Rev. Publ. Health* **21**, 271–307 (2000).
- 976 25. Bakhtsiyarava, M. et al. Modification of temperature-related human mortality by
977 area-level socioeconomic and demographic characteristics in Latin American
978 cities. *Soc. Sci. Med.* **317**, 115526 (2023).
- 979 26. Hu, K. et al. Modifying temperature-related cardiovascular mortality through
980 green-blue space exposure. *Environ. Sci. Ecotechnol.* **20**, 100408 (2024).
- 981 27. Saffari, M. et al. Thermal stress reduction in cool roof membranes using phase
982 change materials (pcm). *Energ. Buildings* **158**, 1097–1105 (2017).
- 983 28. Imran, H. M., Kala, J., Ng, A. W. M. & Muthukumaran, S. Effectiveness of green
984 and cool roofs in mitigating urban heat island effects during a heatwave event in
985 the city of Melbourne in southeast Australia. *J. Clean. Prod.* **197**, 393–405
986 (2018).

-
- 987 29. Yang, J. & Bou-Zeid, E. Should cities embrace their heat islands as shields from
988 extreme cold? *J. Appl. Meteorol. Climatol.* **57**, 1309–1320 (2018).
- 989 30. Krayenhoff, E. S. et al. Cooling hot cities: a systematic and critical review of the
990 numerical modelling literature. *Environ. Res. Lett.* **16**, 053007 (2021).
- 991 31. Wang, Z. H. Compound environmental impact of urban mitigation strategies: Co-
992 benefits, tradeoffs, and unintended consequence. *Sustain. Cities Soc.* **75**, 103284
993 (2021).
- 994 32. Iungman, T. et al. Cooling cities through urban green infrastructure: a health
995 impact assessment of European cities. *The Lancet* **401**, 577–589 (2023).
- 996 33. Macintyre, H. L. & Heaviside, C. Potential benefits of cool roofs in reducing
997 heat-related mortality during heatwaves in a European city. *Environ. Int.* **127**,
998 430–441 (2019).
- 999 34. He, C., He, L., Zhang, Y., Kinney, L P. & Ma, W. Potential impacts of cool and
1000 green roofs on temperature-related mortality in the Greater Boston region.
1001 *Environ. Res. Lett.* **15**, 094042 (2020).
- 1002 35. Oke T.R, Mills, G. & Voogt, J. Urban climates. *Cambridge University Press*
1003 (2017).
- 1004 36. Santamouris, M. Using cool pavements as a mitigation strategy to fight urban
1005 heat island—A review of the actual developments. *Renew. Sust. Energ. Rev.* **26**,
1006 224–240 (2013).
- 1007 37. Rosso, F. et al. New cool concrete for building envelopes and urban paving:
1008 Optics-energy and thermal assessment in dynamic conditions. *Energ. Buildings*
1009 **151**, 381–392 (2017).
- 1010 38. Ramamurthy, P. et al. Influence of subfacet heterogeneity and material properties
1011 on the urban surface energy budget. *J. Appl. Meteorol. Clim.* **53**, 2114–2129

-
- 1012 (2014).
- 1013 39. Zhao, Q. et al. Global, regional, and national burden of mortality associated with
1014 non-optimal ambient temperatures from 2000 to 2019: a three-stage modelling
1015 study. *Lancet Planet. Health* **5**, e415–e425 (2021).
- 1016 40. Gasparri, A. et al. Projections of temperature-related excess mortality under
1017 climate change scenarios. *Lancet Planet. Health* **1**, e360–e367 (2017).
- 1018 41. Martínez-Solanas, È. et al. Projections of temperature-attributable mortality in
1019 Europe: a time series analysis of 147 contiguous regions in 16 countries. *Lancet*
1020 *Planet. Health* **5**, e446–e454 (2021).
- 1021 42. Massaro, E., et al. Spatially-optimized urban greening for reduction of population
1022 exposure to land surface temperature extremes. *Nat. Commun.* **14**, 2903 (2023).
- 1023 43. Tan, J. et al. The urban heat island and its impact on heat waves and human health
1024 in Shanghai. *Int. J. Biometeorol.* **54**, 75–84 (2010).
- 1025 44. Liu, Z. et al. Surface warming in global cities is substantially more rapid than in
1026 rural background areas. *Commun. Earth Environ.* **3**, 219 (2022).
- 1027 45. Zhang, H. et al. Unequal urban heat burdens impede climate justice and equity
1028 goals. *The Innovation* 100488 (2023).
- 1029 46. Keeler, B. L. et al. Social-ecological and technological factors moderate the value
1030 of urban nature. *Nat. Sustain.* **2**, 29–38 (2019).
- 1031 47. Turner, V. K., Middel, A. & Vanos, J. K. Shade is an essential solution for hotter
1032 cities. *Nature* **619**, 694–697 (2023).
- 1033 48. Paschalis, A., Chakraborty, T., Fatichi, S., Meili, N. & Manoli, G. Urban forests
1034 as main regulator of the evaporative cooling effect in cities. *AGU Adv.* **2**,
1035 e2020AV000303 (2021).
- 1036 49. Endreny, T. A. Strategically growing the urban forest will improve our world.

-
- 1037 *Nat. Commun.* **9**, 1160 (2018).
- 1038 50. Jones, B. et al. Future population exposure to US heat extremes. *Nat. Clim.*
1039 *Change* **5**, 652-655 (2015).
- 1040 51. Lüthi, S. et al. Rapid increase in the risk of heat-related mortality. *Nat. Commun.*
1041 **14**, 4894 (2023).
- 1042 52. Baldwin, J. W., Dessy, J. B., Vecchi, A. G. & Oppenheimer, M. Temporally
1043 compound heat wave events and global warming: An emerging hazard. *Earth's*
1044 *Future* **7**, 411–427 (2019).
- 1045 53. Li, X. et al. Mapping global urban boundaries from the global artificial
1046 impervious area (GAIA) data. *Environ. Res. Lett.* **15**, 094044 (2020).
- 1047 54. Kotték, M., Grieser, J., Beck, C., Rudolf, B. & Rubel, F. World map of the
1048 Köppen-Geiger climate classification updated. *Meteorol. Z.* **15**, 259–263 (2006).
- 1049 55. Zhang, T. et al. A global dataset of daily near-surface air temperature at 1-km
1050 resolution (2003–2020). *Earth Syst. Sci. Data Discuss.* 1–18 (2022).
- 1051 56. Eyring, V. et al. Overview of the Coupled Model Intercomparison Project Phase 6
1052 (CMIP6) experimental design and organization. *Geosci. Model Dev.* **9**, 1937-
1053 1958 (2016).
- 1054 57. O'Neill, B. C. et al. The scenario model intercomparison project (ScenarioMIP)
1055 for CMIP6. *Geosci. Model Dev.* **9**, 3461–3482 (2016).
- 1056 58. Muñoz-Sabater, J. et al. ERA5-Land: a state-of-the-art global reanalysis dataset
1057 for land applications. *Earth Syst. Sci. Data* **13**, 4349–83 (2021).
- 1058 59. Chen, J. et al. Global 1 km × 1 km gridded revised real gross domestic product
1059 and electricity consumption during 1992–2019 based on calibrated nighttime light
1060 data. *Sci. Data* **9**, 202 (2022).
- 1061 60. Dobson, J. E. LandScan: A global population database for estimating populations

-
- 1062 at risk. *Photogramm. Eng. Rem. S.* **66**, 849–857 (2000).
- 1063 61. Gao, J. Downscaling global spatial population projections from 1/8-degree to 1-
1064 km grid cells. National Center for Atmospheric Research, Boulder, CO, USA.
1065 1105 (2017).
- 1066 62. Krummenauer, L. et al. Global drivers of minimum mortality temperatures in
1067 cities. *Sci. Total Environ.* **695**, 133560 (2019).
- 1068 63. Gesch, D. B., Verdin, K. L. & Greenlee, S. K. New land surface digital elevation
1069 model covers the Earth. *Eos, Transactions American Geophysical Union* **80**, 69-
1070 70 (1999).
- 1071 64. Menashe, D. S. & Friedl, M. A. User guide to collection 6 MODIS land cover
1072 (MCD12Q1 and MCD12C1) product. Retrieved from
1073 https://lpdaac.usgs.gov/documents/101/MCD12_User_Guide_V6.pdf (2018).
- 1074 65. Gasparri, A. et al. Small-area assessment of temperature-related mortality risks
1075 in England and Wales: a case time series analysis. *Lancet Planet. Health* **6**, e557-
1076 e564 (2022).
- 1077 66. Achebak, H., Devolder, D., Ingole, V. & Ballester, B. Reversal of the seasonality
1078 of temperature-attributable mortality from respiratory diseases in Spain. *Nat.*
1079 *Commun.* **11**, 1-9 (2020).
- 1080 67. Huber, V. et al. Temperature-related excess mortality in German cities at 2 °C and
1081 higher degrees of global warming. *Environ. Res.* **186**, 109447 (2020).
- 1082 68. Lee, W. H. et al. An investigation on attributes of ambient temperature and
1083 diurnal temperature range on mortality in five east-Asian countries. *Sci. Rep-UK.*
1084 **7**, 1-9 (2017).
- 1085 69. Imhoff, M. L., Zhang, P., Wolfe, E. R. & Bounoua, L. Remote sensing of the
1086 urban heat island effect across biomes in the continental USA. *Remote Sens.*

-
- 1087 *Environ.* **114**, 504–513 (2010).
- 1088 70. Yao, R., Wang, L., Huang, X., Gong, W. & Xia, X. Greening in rural areas
1089 increases the surface urban heat island intensity. *Geophys. Res. Lett.* **46**, 2204–
1090 2212 (2019).
- 1091 71. Peng, S. et al. Surface urban heat island across 419 global big cities. *Environ. Sci.*
1092 *Technol.* **46**, 696–703 (2012).
- 1093 72. Anderson, B. G. & Bell, M. L. Weather-related mortality: how heat, cold, and
1094 heat waves affect mortality in the United States. *Epidemiology* **20**, 205–13
1095 (2009).
- 1096 73. Guo, Y. et al. Global variation in the effects of ambient temperature on mortality:
1097 a systematic evaluation. *Epidemiology (Cambridge, Mass.)* **25**, 781 (2014).
- 1098 74. Yin, Q., Wang, J., Ren, Z., Li, J. & Guo, Y. Mapping the increased minimum
1099 mortality temperatures in the context of global climate change. *Nat. Commun.* **10**,
1100 4640 (2019).
- 1101 75. Tewari, M. et al. Interaction of urban heat islands and heat waves under current
1102 and future climate conditions and their mitigation using green and cool roofs in
1103 New York City and Phoenix, Arizona. *Environ. Res. Lett.* **14**, 034002 (2019).
- 1104 76. Synnefa, A., Dandou, A., Santamouris, M., Tombrou, M. & Soulakellis, N. On the
1105 use of cool materials as a heat island mitigation strategy. *J. Appl. Meteorol. Clim.*
1106 **47**, 2846–2856 (2008).
- 1107 77. Zinzi, M. & Agnoli, S. Cool and green roofs. An energy and comfort comparison
1108 between passive cooling and mitigation urban heat island techniques for
1109 residential buildings in the Mediterranean region. *Energ. Buildings* **55**, 66–76
1110 (2012).

-
- 1111 78. Marando, F. et al. Urban heat island mitigation by green infrastructure in
1112 European functional urban areas. *Sustain. Cities. Soc.* **77**, 103564 (2022).
- 1113 79. Schwaab, J. et al. The role of urban trees in reducing land surface temperatures in
1114 European cities. *Nat. Commun.* **12**, 6763 (2021).
- 1115 80. Isaac, M. & Van Vuuren, D. P. Modeling global residential sector energy demand
1116 for heating and air conditioning in the context of climate change. *Energy Policy*
1117 **37**, 507–521 (2009).
- 1118 81. Lobaccaro, G. & Acero, J. A. Comparative analysis of green actions to improve
1119 outdoor thermal comfort inside typical urban street canyons. *Urban Climate* **14**,
1120 251-267 (2015).
- 1121 82. Jandaghian, Z. & Akbari, H. Increasing urban albedo to reduce heat-related
1122 mortality in Toronto and Montreal, Canada. *Energ. Buildings* **237**, 110697 (2021).
- 1123 83. Manoli, G. et al. Magnitude of urban heat islands largely explained by climate
1124 and population. *Nature* **573**, 55–60 (2019).
- 1125 84. Venter, Z. S., Chakraborty, T. & Lee, X. Crowdsourced air temperatures contrast
1126 satellite measures of the urban heat island and its mechanisms. *Sci. Adv.* **7**,
1127 eabb9569 (2021).
- 1128 85. Zhao, L., Lee, X., Smith, B. R. & Oleson, K. Strong contributions of local
1129 background climate to urban heat islands. *Nature* **511**, 216–219 (2014).
- 1130 86. Jacobson, M. Z. & Hoesung, J. E.T. Effects of urban surfaces and white roofs on
1131 global and regional climate. *J. Climate* **25**, 1028–1044 (2012).
- 1132 87. Virk, G. et al. Microclimatic effects of green and cool roofs in London and their
1133 impacts on energy use for a typical office building. *Energ. Buildings* **88**, 214–228
1134 (2015).

-
- 1135 88. Madanian, M. et al. The study of thermal pattern changes using Landsat-derived
1136 land surface temperature in the central part of Isfahan province. *Sustain. Cities*
1137 *Soc.* **39**, 650–661 (2018).
- 1138 89. Nirandjan, S., Koks, E. E., Ward, P. J. & Aerts, J. C. A spatially-explicit
1139 harmonized global dataset of critical infrastructure. *Scientific Data* **9**, 150 (2022).
- 1140 90. Kummu, M., Taka, M. & Guillaume, J. H. Gridded global datasets for gross
1141 domestic product and Human Development Index over 1990–2015. *Scientific*
1142 *data*, **5**, 1-15 (2018).
- 1143 91. Wang, J. et al. Significant effects of ecological context on urban trees' cooling
1144 efficiency. *ISPRS J. Photogramm. Remote Sens.* **159**, 78–89 (2020).
- 1145 92. Gatti, P. L. Probability theory and mathematical statistics for engineers. CRC
1146 Press. 2004.